Acute retinal injury and the relationship between nerve growth factor, Notch1 transcription and short-lived dedifferentiation transient changes of mammalian Müller cells

Qian Jian, Zui Tao, Yaochen Li *, Zheng Qin Yin *

Southwest Hospital/Southwest Eye Hospital, Third Military Medical University, Chongqing 400038, China
Key Lab of Visual Damage and Regeneration & Restoration of Chongqing, Chongqing 400038, China

ARTICLE INFO

ABSTRACT

Our aim is to define related molecular events on how dormant Müller glia cells re-enter the cell cycle, proliferate and produce new retinal neurons from initial injury to glial scar formation. Sodium iodate ($NaIO_3$) was used to induce acute retinal injury. Long-Evans rats were administered with $NaIO_3$ or phosphate-buffered saline by intraperitoneal injection. The proliferation, dedifferentiation and neurogenesis of Müller cells were analyzed by double-labeled fluorescence immunohistochemistry with primary antibodies – against Müller cells and specific cell markers. Possible molecules that limit the regenerative potential of Müller cells were also determined by immunofluorescence staining, quantitative RT-PCR, protein array, ELISA and Western blot. In the first 3–7 days after $NaIO_3$ administration, Müller cells were activated and underwent a fate switch, including transient proliferation, dedifferentiation and neurogenesis. Nerve growth factor (NGF) signaling concomitantly increased with the downregulation of $p27^{Kip1}$ in Müller cells, which may promote Müller cells to re-enter the cell cycle. The transient increase of NGF signaling and the transient decrease of Notch signaling inhibited *Hes1*, which might enhance the neuronal differentiation of dedifferentiated Müller cells and suppress gliosis. Upregulated Notch and decreased NGF expressions limit dedifferentiation and neurogenesis, but induces retinal Müller cell gliosis at a later stage. We conclude that transient NGF upregulation and Notch1 downregulation may activate the transient proliferation, dedifferentiation and neurogenesis of Müller cells during $NaIO_3$-induced acute retinal injury; which could be a therapeutic target for overcoming Müller cell gliosis. Such therapy could be potentially used for treating retinal-related diseases.

© 2015 Elsevier Ltd. All rights reserved.

1. Introduction

Müller glial cells that transverse most of the retina are known to be anatomically and functionally essential for retinal development and homeostasis (Bringmann et al., 2006; Goldman, 2014). Previous studies revealed that Müller cells act as endogenous stem cells in non-mammalian vertebrate retinas to regenerate retinal neurons after injury, such as in zebrafish (Bernardos et al., 2007; Nelson et al., 2013). Rodent retinal Müller cells also have a gene expression profile similar to retinal progenitor cells (Blackshaw et al., 2004; Karl & Reh, 2010). However, in response to injury and retinal diseases, mammalian Müller cells undergo proliferation and gliosis that can lead to permanent loss of vision, unlike amphibians and fish (Fariss, Li, & Milam, 2000; Kimura et al., 1999; Li, Possin, & Milam, 1995; Taomoto et al., 1998; WHO, 2007).

Excessive activation and proliferation of Müller cells residing in the subretinal space eventually form glial scars with outer segment debris, exacerbating photoreceptor apoptosis (Fletcher, 2000; Pierce et al., 1999). From these observations, we can conclude that Müller cells undergo a complex and dynamic process in the course of cell injury and repair. Thus, Müller cell gliosis has become an important target for visual regeneration research in related retinal diseases (Huo et al., 2012).

Over the last few decades, significant progress has been made to elucidate the molecular basis of retinal regeneration and repair; but the mechanisms involving Müller cell regeneration in the adult mammalian retinas are still unknown (Fischer & Reh, 2001; Ooto et al., 2004). Environmental stimuli or endocrine signals (Nguyen, Nioi, & Pickett, 2009) may cause regulatory protein modifications

---

* Corresponding authors at: Southwest Hospital/Southwest Eye Hospital, Third Military Medical University, Chongqing 400038, China. Fax: +86 23 65460711 (O) (Y. Li), +86 23 65460711 (O) (Z.Q. Yin).

E-mail addresses: yaochenli-2004@163.com (Y. Li), qinzyin@aliyun.com (Z.Q. Yin).

(Paul, 2008) and elicit a cascade of intracellular signals (Los et al., 2009) that result in gene expression regulation. This means that complex and dynamic Müller cell changes depend on the "open state" or "close state" of chromatin, which is followed by the initiation or repression of gene transcription (Weng, Araki, & Subedi, 2012). Unfortunately, few reports focused on the in vivo dynamic changes of diverse molecular events associated with Müller cell proliferation, dedifferentiation and neurogenesis.

Acute rat retinal injury model induced by NaIO$_3$ is characterized by regional and selective retinal pigment epithelium (RPE) degeneration and atrophy, and then followed by the degeneration of photoreceptors. NaIO$_3$-induced RPE injury is one of widely used models to study diseases such as retinitis pigmentosa and age-related macular degeneration (Machalinska et al., 2013; Tao et al., 2013). In this study, we used a NaIO$_3$-induced acute retinal injury model to define molecular events correlated with the re-entry of dormant Müller glia into the cell cycle, their proliferation and the production of retinal neurons from initial injury to glial scar formation. The data obtained from this study may allow us to define therapeutic targets.

2. Materials and methods

2.1. Materials

NaIO$_3$ in saline was obtained from Sigma Chemical (St. Louis, MO).

Mouse anti-rhodopsin and rabbit anti-PH3, anti-SOX2, anti-GFAP, anti-TrkA and anti-Notch1 were obtained from Abcam (Cambridge, MA, USA). Rabbit anti-PAX6 and anti-crx, and sheep anti-Delta were obtained from Santa Cruz Biotechnology, Inc. (Dallas, TX, USA). Mouse anti-BrdU was obtained from Millipore (Billerica, MA, USA). Mouse anti-CD44, anti-GAPDH and anti-p27^{Kip1} were obtained from Cell Signaling Technology (Danvers, MA, USA). A RayBio® Biotin Label-based Rat Antibody Array 1 (AAR-BLG-1-8) was obtained from RayBiotech, Inc. (Norcross, GA, USA). Slides were obtained from Corning Incorporated (Corning, NY, USA). HiLytePlus™ 555 (Cy3 equivalent) was obtained from AnaSpec (Freemont, CA, USA). PrimeScript™ RT reagent Kit was obtained from Takara Bio. Inc. (Tech, Otsu, Shiga, Japan). TRIzol® reagent and a TURBO DNA-free™ Kit were obtained from Life Technologies (Grand Island, NY, USA).

2.2. Animal model and NaIO$_3$ administration

All experiments were approved by the Animal Ethics Committee of the Southwest Hospital in Chongqing, China and adhered to the EU Directive 2010/63/EU for animal experiments, as well as Uniform Requirements for manuscripts submitted to Biomedical journals. Long-Evans rats (LE rats, 35–40 days-old) were used in the study. A sterile NaIO$_3$ saline solution (1% NaIO$_3$ in PBS) was intraperitoneally injected (50 mg/kg body weight), into rats that were restrained briefly (TV-150, Braintree Scientific, Braintree, MA) as previously described (Kiuchi et al., 2002; Li et al., 2007; Tao et al., 2013). Both phosphate buffered saline (PBS) treated rats and untreated rats served as controls. Eyes were harvested on days 3, 7, 14, and 28 after NaIO$_3$ administration.

2.3. Immunofluorescence staining

To observe retinal proliferation, rats were intraperitoneally injected twice with bromo-deoxyuridine (BrdU) (100 mg/kg) every four hours, anesthetized with pentobarbital sodium (50 mg/kg, intraperitoneally) and sacrificed two hours after the last BrdU injection, as previously described (Jian et al., 2009; Tao et al., 2013). Eye cups were fixed with 4% paraformaldehyde in PBS for two hours and immersed in 30% sucrose in PBS for 16 h. A freezing microtome was used to cut Sagittal sections of eye cups to a thickness of 8 μm. The sections were stained with hematoxylin and eosin, and examined microscopically.

Immunofluorescence staining of frozen sections were performed as described previously (Jian, Li, & Yin, 2015; Jian et al., 2009; Wan et al., 2007; Xu et al., 2013). The sections were briefly incubated with a primary antibody overnight at 4 °C: mouse anti-BrdU, rabbit anti-PH3, rabbit anti-SOX2, rabbit anti-PAX6, rabbit anti-crx, mouse anti-rhodopsin, mouse anti-CD44, rabbit anti-GFAP, mouse anti-p27^{Kip1}, rabbit anti-TrkA, rabbit anti-Notch1 or sheep anti-Delta. The sections were then incubated for one hour at room temperature with a secondary antibody. Fluorescence was visualized by either an Olympus microscope OP70 (Olympus Microscopy, Japan) or a confocal microscope Leica TCS SP50 (Leica Microsystems, Wetzlar, Germany). The somata of Müller cells are generally localized in the INL, and the cytoplasm, membrane and processes of Müller cell were positive to the cell markers CRALBP or GS (green). The other markers (red), such as proliferation markers (nuclei), stem cell/progenitor markers (nuclei), photoreceptor marker (cytoplasm and membrane) and signaling molecule markers (the cytoplasm, membrane or nuclei), were double stained with Müller cell markers CRALBP or GS. All the double-stained cells (yellow) in the INL of the retina were visualized and quantified using a confocal microscope Leica TCS SP50 (Leica Microsystems, Wetzlar, Germany). The double-labeled cells were confirmed with orthogonal views in the z axis, photographed and then counted. To avoid counting the same cell in more than one section, serial cross sections of the retina were made, and every sixth section (48 μm apart) was observed and counted. The number of double-labeled cells in the retinas were counted at constant magnification as shown in the figures. For each section, three separate retinal fields were examined: two fields in the opposite ambits, one in the posterior pole avoiding the optic nerve. The average number of double-labeled cells per field in each retinal section was used for statistics. Data from three retinal sections from six rats were selected for statistical analysis ($n = 18$). Photoshop CS 8.01 (Adobe Systems, Inc., San Jose, CA, USA) was used to create the figures.

2.4. Antibody chip technology

Retinal lysates from NaIO$_3$- and PBS-treated rats were filtered through a 0.22 μm syringe filter. A RayBio® Biotin Label-based Rat Antibody Array 1 was used in the glass slide format and 90 rat proteins were detected including: adipokines, adhesion molecules, angiogenic factors, binding proteins, chemokines, cytokines, growth and differentiation factors, inhibitors, matrix metalloproteases, and soluble receptor proteins. A contact arrayer was used to print the antibodies (200 μg/ml, approximately) Corning slides. Captured antibody diluents were included as negative controls in the printed array. Diluted biotin-conjugated IgG and anti-streptavidin were included as positive controls. After blocking, the chips were incubated with 400 μl of retinal lysate sample at room temperature for two hours. Protein chips were incubated with streptavidin-conjugated fluorescent dye, HiLytePlus™ 555 at room temperature for one hour. After removing excess streptavidin dye, fluorescence was measured using a GenePix™ 4000B laser scanner (Axon Instruments, Sunnyvale, CA, USA).

2.5. Enzyme-linked immunosorbent assay (ELISA) of whole retina lysates

Retinal lysates of NaIO$_3$- and PBS-treated rats were filtered through a 0.22 μm syringe filter. ELISA was used to quantify nerve

growth factor (NGF) concentration in retinas according to the manufacturer's instructions (R & D Systems, Minneapolis, MN, USA). Optical density was measured within 30 min at a wavelength of 450 nm.

2.6. Quantitative real-time PCR

Globes were enucleated and the retinas of NaIO$_3$- and PBS-treated rats were isolated and frozen in liquid nitrogen according to our published protocol (Jian et al., 2009; Jian, Li, & Yin, 2015; Li et al., 2012). TRIzol® reagent was used to isolate total RNAs according to manufacturer's instructions. A TURBO DNA-free™ Kit was used to remove contaminating DNAs. In a 20 μl reaction mixture, total RNA (2 μg) was used to synthesize cDNAs using a PrimeScript™ RT Kit, following the manufacturer's instructions (Bio-Rad 5-Color System, Bio-Rad Laboratories, Hercules, CA, USA). The different gene transcripts were amplified using primers, as follows: *Cyclin D1*: 5′-AGA GGC GGA TGA GAA CAA GCA GAT-3′ and 5′-TCT GGA AAG AAA GTG CGT TGT GCG-3′; *PCNA*: 5′-AAAGCCACTCCAC TGTCTCCTACA-3′ and 5′-TGGCATCTCAGAAGCGATCGTCAA-3′; *Hes1*: 5′-CAA CAC GAC ACC GGA CAA ACC AAA-3′ and 5′-TGG AAT GCC GGG AGC TAT CTT TCT-3′; and *GAPDH*: 5′-AGACAGCCGCAT CTTCTTGT-3′ and 5′-TGATGGCAACAATGTCCACT-3′. Relative to the control rats, a change in target gene expression was calculated in NaIO$_3$-treated rats as follows: fold change = $2^{-(\Delta CT,Tg - \Delta CT,control)}$. The PCR cycling parameters used were: five minutes at 94 °C, (30 s at 94 °C, 30 s at 63 °C, 30 s at 72 °C) × 35, 10 min at 72 °C, and 4 °C thereafter.

2.7. Western blot analysis

Western blot analysis were performed, as previously described (Jian, Li, & Yin, 2015; Li et al., 2012; Tao et al., 2013). To detect the protein expression levels of Notch1, the samples (50 μg of protein/lane) from the retinas of NaIO$_3$- and PBS-treated rats were loaded onto a 12% sodium dodecyl sulfate (SDS)–polyacrylamide gel and electrophoresed for 40 min at 120 V. Proteins from the gel were transferred onto blocked nitrocellulose membranes at 120 V for 70 min. The membranes were incubated overnight at 4 °C with primary antibodies, rabbit anti-Notch1 and mouse anti-GAPDH. Then, different secondary antibodies were incubated with the membranes for one hour at room temperature, while shaking. Finally, Notch1 and glyceraldehyde 3-phosphate dehydrogenase (GAPDH) bands on the nitrocellulose membranes were scanned and quantified using an Odyssey infrared imaging system (Bio-rad Laboratories, Hercules, CA, USA) with Odyssey Application software V1.2.15. The relative level of Notch1 was obtained by calculating the ratio of Notch1 to GAPDH using densitometry.

2.8. Statistics

According to the double blinded method, counting was done by a well-trained technician who was not aware of the experimental conditions. For immunofluorescence staining, data from three retinal sections from six rats were selected for statistical analysis (*n* = 18). For qPRC, ELISA, and Western blot analyses, ten retinas from five rats were harvested and five samples were prepared (*n* = 5). For protein chip studies, six retinas from three rats were harvested and three samples were prepared (*n* = 3). All experiments were repeated three times. Data were presented as the mean ± the standard error of the mean. Differences between means were tested using a non-parametric test, *t*-test or ANOVA using SPSS 11.0 software (IBM Corporation, Armonk, New York, USA). A *P* < 0.05 was considered significant.

3. Results

3.1. Retinal morphological changes following NaIO$_3$-induced retinal injury

Over a one month period, untreated rats and PBS-treated rats (Fig. 1A) showed normal retinal structures without any differences between them or between the time-matched groups. NaIO$_3$-induced structural changes were stable, remarkable and time dependent. After NaIO$_3$ completely destroyed the RPE by the 3rd day, a thin layer of melanin was released along Bruch's membrane and replaced the RPE (Fig. 1B). After NaIO$_3$ delivery, the thicknesses of the outer nuclear layer (ONL) and inner nuclear layer (INL) were very unevenly distributed on the 7th day. The most typical characteristic of the INL was segmental thickening (Fig. 1C) and extension towards the outer nuclear layer, beyond the outer plexiform layer (OPL). After NaIO$_3$ administration, the thickness of the ONL significantly decreased on the 14th and 28th day; and the inner and outer photoreceptor segments were shortened (Fig. 1D and E). The morphological changes of the NaIO$_3$-induced rat retina were consistent with published reports (Machalinska et al., 2010). The drastic and predominant reduction in retinal thickness presented an obvious proliferative state, due to the progressive loss of photoreceptors and segmental cells in the INL.

3.2. Re-entry of Müller glial cells into the cell cycle from a quiescent G0 state following NaIO$_3$-induced retinal injury

Rats were intraperitoneally injected with BrdU two hours before harvesting the eyes. Combined immunofluorescence staining against Müller glia marker CRALBP (cellular retinaldehyde-binding protein) and DNA replication marker BrdU showed that a few Müller glia-derived progenitors started to express strong positive proliferative signals in the injured retinas on the 3rd day; but a few double positive cells were seen in the control retinas (Fig. 2A). For NaIO$_3$-induced retinal injuries, BrdU and CRALBP double positive cells – per field – were significantly increased (10.3 ± 4.4, *P* < 0.001) three days after NaIO$_3$ administration, compared with the value (2.8 ± 2.5) for control rat retinas. After NaIO$_3$ administration, the number of double positive cells in NaIO$_3$-induced retinal injuries reached its peak on the 7th day (Fig. 2B, enlarged in C), compared with controls (*P* < 0.001); which sharply declined afterwards. There were no significant differences between the two groups on the 14th and 28th day after NaIO$_3$ administration (*P* > 0.05) (Fig. 2D and I). Therefore, we believe that NaIO$_3$-induced retinal injury caused the level of BrdU-positive proliferative cells to increase. These results did not necessarily conclude that visibly positive cells were dividing because during DNA repair or S-phase DNA synthesis, BrdU can be incorporated. To confirm that Müller cells were dividing, we used an antibody against phosphorylated histone 3, PH3 which is a proliferation marker that is expressed from late G2 to anaphase; and we found an expression pattern similar to BrdU. After NaIO$_3$ administration, the number of double positive cells significantly increased on the 3rd, 7th and 14th day, compared with control retinas (Fig. 2E, F, H and J, enlarged in G).

3.3. Stem/progenitor cell marker expressions in Müller cells increased following NaIO$_3$-induced retinal injury

The retina was double stained for CRALBP, a marker for RPE and Müller glial cells, and stem cell/progenitor cell markers SOX2 or PAX6. We found that stem cell/progenitor marker expressions, such as SOX2 (Fig. 3A, B, D, enlarged in C) and PAX6 (Fig. 3E, F, H, enlarged in G), increased in the retinas of NaIO$_3$-treated rats; which co-localized more with CRALBP compared with the PBS-treated
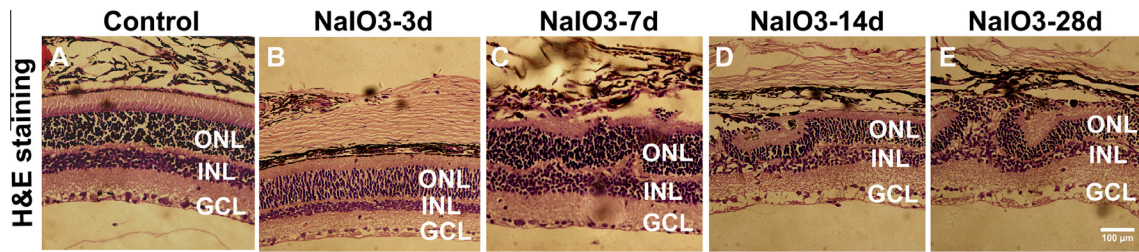
Fig. 1. Morphological changes of the NaIO$_3$-induced rat retinal acute injured model. Comparison of the retinal histological structure by H&E staining in retinal vertical sections between PBS-treated and NaIO$_3$-treated retinas at various time-points: (A) represents the control retina time-matched on the 3rd day; (B–E) represent NaIO$_3$-induced retinal injuries on the 3rd, 7th, 14th and 28th day after NaIO$_3$ administration. ONL: outer nuclear layer; INL: inner nuclear layer; GCL: ganglion cell layer; scale bar = 100 μm.
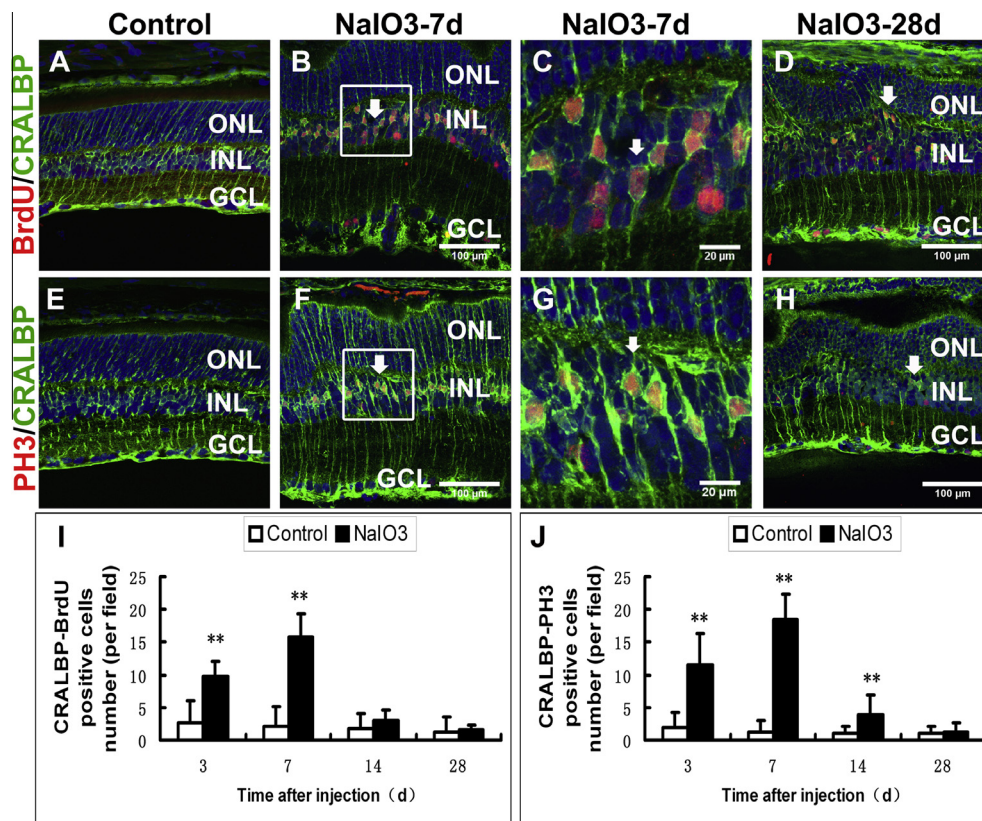

Fig. 2. Results of NaIO$_3$ administration in increased Müller cell proliferative ability in vivo. Double-labeling immunofluorescence staining was performed on frozen retinal tissue sections treated with NaIO$_3$ and with CRALBP (green) and BrdU (red) (A–D) or PH3 (red) (E–H) antibodies; PBS-treated retinal tissues were used as controls. The proportion of LE rat Müller cells treated with NaIO$_3$ in BrdU-positive or PH3-positive Müller cells showed a rapid increase during the early processing stages of injury; and reached its peak on the 7th day after injury, compared with PBS-treated retinas (I and J). The arrows in (C) and (G) show highly magnified BrdU and PH3 positive Müller's cells, respectively. Thereafter, the number of BrdU-positive or PH3-positive Müller cells gradually reduced over time (D and H). ONL: outer nuclear layer; INL: inner nuclear layer; GCL: ganglion cell layer; arrows indicate double positive cell labeling; $n = 18$, $^*P < 0.05$, $^{**}P < 0.01$; scale bar = 100/20 μm. (For interpretation of the references to color in this figure legend, the reader is referred to the web version of this article.)

groups. After NaIO$_3$ administration, the number of positive Müller cells for the two types of stem cell/progenitor markers were significantly more than that of the time-matched control groups on the 3rd, 7th, and 14th day, especially on 3rd day (Fig. 3I and J). With injury, the number of positive Müller cells for the two types of stem/progenitor markers decreased on the 28th day after NaIO$_3$ administration; and no significant difference was found between the NaIO$_3$-treated and control groups(Fig. 3D, H and I, J).

3.4. A subset of Müller cells in NaIO$_3$-induced retinal injury exhibited neurogenesis abilities

We double stained the retinal sections for crx, which is an early photoreceptor marker (Fig. 4A–D and I), rhodopsin, a mature photoreceptor marker (Fig. 4E–H and J) and GS, glutamine synthetase, a marker for Müller cells. Interestingly, three days after NaIO$_3$ administration, we found that a few cells were positively stained for crx and rhodopsin in the INL (Fig. 4B and F, arrows; enlarged in C and G, respectively), which colocalized with GS – but no positive signals were observed in the INL of control retinas. Thereafter, the number of double positive cells in the INL was gradually reduced with time (Fig. 4I and J); and individual double positive cells were still observed in injured retinas on the 28th day (Fig. 4H).

3.5. Müller cells underwent glial fates after injury at later stages

To provide a more specific analysis for Müller cells, we used GFAP and CD44 antibodies (Fig. 5A–E); since CD44 is highly
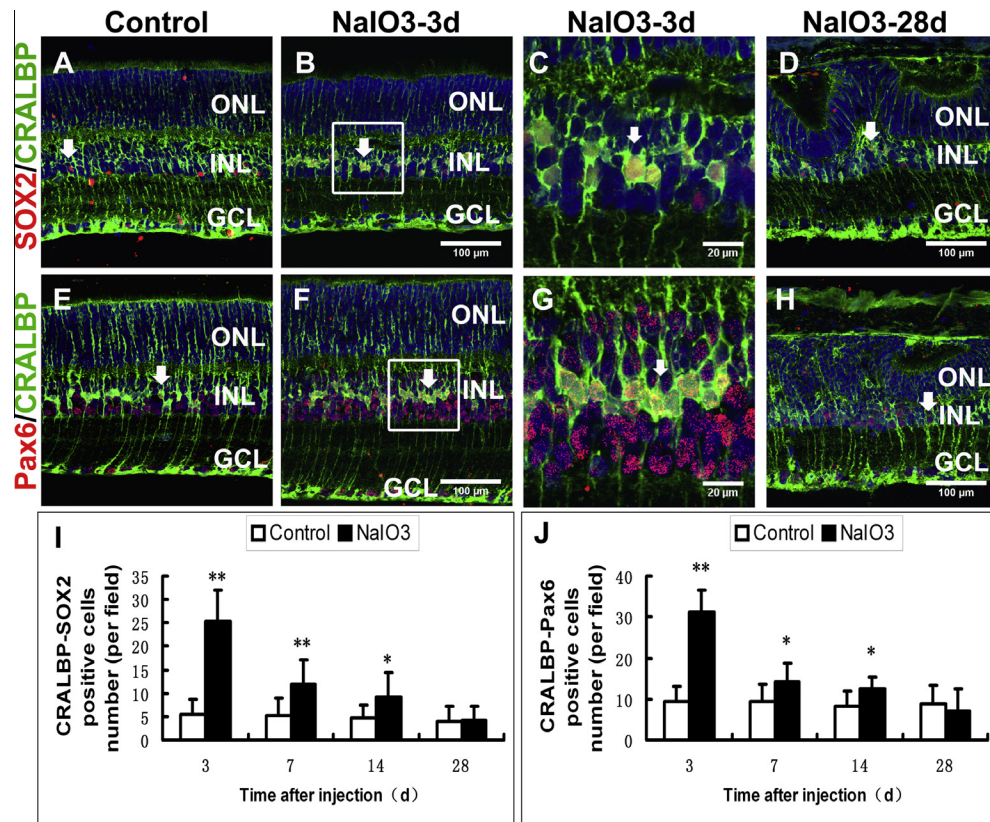
Fig. 3. Results of $NaIO_3$ administration in the enhanced dedifferentiation ability of Müller cells in vivo. Double-labeling immunofluorescence staining of frozen retinal tissue sections treated with $NaIO_3$, as well as with CRALBP (green) and SOX2 (red) (A–D) or PAX6 (red) (E–H) are shown. PBS-treated retinal tissues are used as controls. The number of SOX2 or PAX6 positive Müller cells rapidly increased during the early processing stages of injury in LE rats treated with $NaIO_3$; and reached its peak on the 3rd day after injury, compared with control retinas (I and J). The arrows in (C) and (G) show highly magnified SOX2 and PAX6 positive Müller's cells, respectively. Thereafter, the number of SOX2 or PAX6 positive Müller cells gradually reduced over time. On the 28th day after injury, no significant difference was found between the two groups – pertaining to the number of double positive Müller cells (D and H). ONL: outer nuclear layer; INL: inner nuclear layer; GCL: ganglion cell layer; arrows indicate double positive cell labeling; $n = 18$, $^*P < 0.05$, $^{**}P < 0.01$; scale bar = 100/20 µm. (For interpretation of the references to color in this figure legend, the reader is referred to the web version of this article.)

expressed in the apical microvilli of Müller glial cells – which form the outer limiting membrane of the retina (Rich et al., 1995; Goldman, 2014). We examined the spatial expressions of CD44 and GFAP in Müller cells at various time-points after $NaIO_3$ administration (In normal retinas, astrocytes; but a few Müller cells are labeled with anti-GFAP). Labeling can be observed from activated Müller cells as detected by immunostaining of frozen retinal sections. In normal retinas, we could see a continuous and intact CD44 positive outer limiting membrane, and no GFAP positive signals were observed. In contrast, we observed that GFAP started expressing on the 3rd day of post-injury (Fig. 5B), compared with control retinas (Fig. 5A). Afterwards, GFAP expressions significantly increased in $NaIO_3$-treated retinas, which were confined to the injured retinal area (Fig. 5C–E). Interestingly, GFAP-expressing proliferative and hyperplasic Müller cells became thicker at the injured site, and extended into the ONL; which even penetrated the subretinal space, after seven days of $NaIO_3$ administration. An increase in GFAP expression level was observed as time progressed. We also noted that the CD44-positive outer limiting membrane in the retinas started disrupting from the 7th day to 28th day after $NaIO_3$ delivery (Fig. 5C–E; arrows). The outer processes of GFAP-immunoreactive Müller glial cells were present in the disrupted outer limiting membrane regions, and often extended beyond the outer limiting membrane.

3.6. Downregulation of p27^{Kip1} following $NaIO_3$-induced retinal injury

We found that $p27^{Kip1}$ was expressed in the INL, consistent with the Müller cells that were indicated by GS immunoreactivity

(Fig. 6A). In contrast, retinas from the treated group dramatically exhibited a decrease of more than 50% in the proportion of $p27^{Kip1}$-immunoreactive cells on the 3rd day (Fig. 6B and E), compared with that of the control group. A slight increase in the relative amount of $p27^{Kip1}$ immunoreactive cells was found from the 7th to the 28th day (Fig. 6C and E, enlarged in D) after $NaIO_3$ injection; but the proportions were still lower than that of control retinas.

3.7. Cyclin D1 and PCNA were transiently upregulated following $NaIO_3$-induced retinal injury

Quantitative RT-PCR results revealed a significant increase of *Cyclin D1* mRNA expression levels in $NaIO_3$-treated rat retinas, compared with control retinas; especially on the 3rd and 7th day after $NaIO_3$ administration (Fig. 6F). The level of *Cyclin D1* mRNA peaked on the 3rd day after $NaIO_3$ administration. Then, *Cyclin D1* mRNA levels progressively declined with time. No statistical significant difference was found in *Cyclin D1* mRNA levels between the two groups (Fig. 6F) on the 14th day after $NaIO_3$ administration.

Proliferation cell nuclear antigen (*PCNA*) mRNA expression levels were also detected by quantitative RT-PCR (Fig. 6G). The result showed that the expression patterns of *PCNA* mRNA after $NaIO_3$ administration, at all time-points, were similar to that of *Cyclin D1* mRNA. Thus, we believe that following $NaIO_3$ stimulation, *Cyclin D1* was upregulated. Furthermore, *Cyclin D1* upregulation led to the activation of downstream biochemical events, including *PCNA* expression.
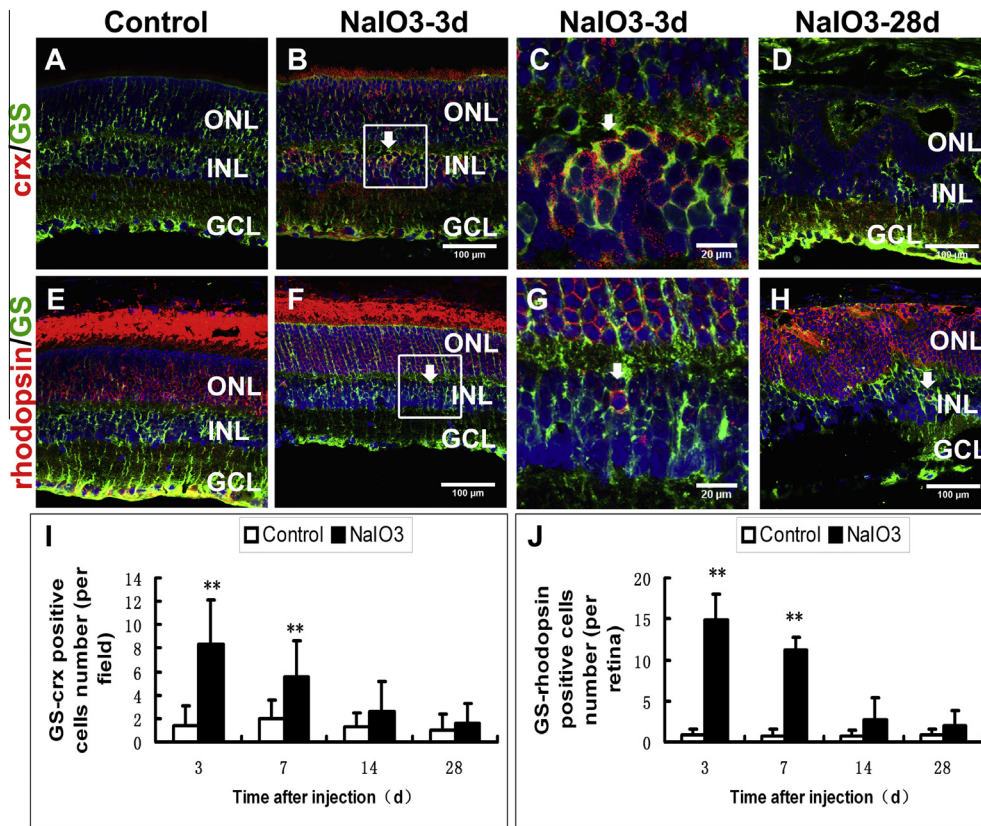
Fig. 4. Results of NaIO$_3$ administration in Müller cell neurogenesis in vivo. Double-labeling immunofluorescence staining was performed on frozen retinal tissue sections treated with NaIO$_3$ and with GS (green) and crx (red) (A–D) or rhodopsin (red) (E–H); PBS-treated retinal tissues were used as controls. The number of crx and rhodopsin positive Müller cells rapidly increased during the early processing stages of injury in LE rats treated with NaIO$_3$; and reached its peak on the 3rd day after injury, compared with control retinas (I and J). The arrows in (C) and (G) show highly magnified crx and rhodopsin positive Müller's cells, respectively. Thereafter, the number of crx and rhodopsin positive Müller cells rapidly reduced over time (D and H). ONL: outer nuclear layer; INL: inner nuclear layer; GCL: ganglion cell layer; arrows indicate double positive cell labeling; $n = 18$, $^*P < 0.05$, $^{**}P < 0.01$; scale bar = 100/20 μm. (For interpretation of the references to color in this figure legend, the reader is referred to the web version of this article.)
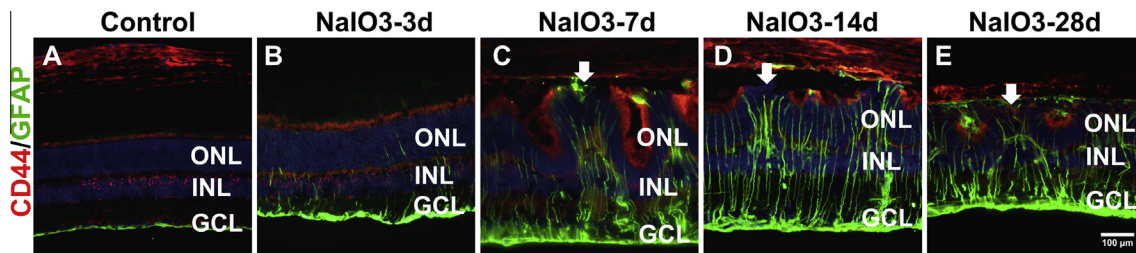

Fig. 5. Comparison of Müller cell glial activation after injury. (A–E) Shows double-labeling immunofluorescence staining with antibodies against CD44 (red) and GFAP (green). The results show that while GFAP expression was gradually upregulated after NaIO$_3$ administration, the continued CD44-positive outer limiting membrane was disrupted (shown by the arrow); enabling the hyperplastic and proliferative processes of Müller cells to extend into the subretinal space. ONL: outer nuclear layer; INL: inner nuclear layer; GCL: ganglion cell layer; arrows indicate double positive cell labeling; scale bar = 100 μm. (For interpretation of the references to color in this figure legend, the reader is referred to the web version of this article.)

3.8. NGF and NGF receptor, TrkA were transiently upregulated following NaIO$_3$-induced retinal injury

Antibody chip results showed that increased NGF expressions in NaIO$_3$-treated retinas were transient and detectable only on the 3rd day after treatment (Fig. 7A–D). However, ELISA analysis revealed that the expression level NGF increased significantly on the 3rd day, and decreased on the 7th day after treatment compared to control retinas (Fig. 7E). NGF diluted in assay diluents (block and sample buffer) was used to make a linear standard curve ($R^2 = 0.9904$). Furthermore, to test whether increased NGF

levels affect Müller cells through neurotrophic tyrosine kinase receptor type 1 (TrkA), double-labeling immunofluorescence staining against GS and TrkA was performed on the frozen retinal sections. The test revealed that a portion of TrkA-positive signals could co-localize with GS expressions in Müller cells. The number of double positive signals were significantly higher in retinas from the NaIO$_3$-treated rats, compared with retinas from the control group (Fig. 7G); reaching a peak value on the 3rd day after NaIO$_3$ administration (Fig. 7H and F, enlarged in I). Then, the number of double positive Müller cells gradually decreased (Fig. 7J and F).
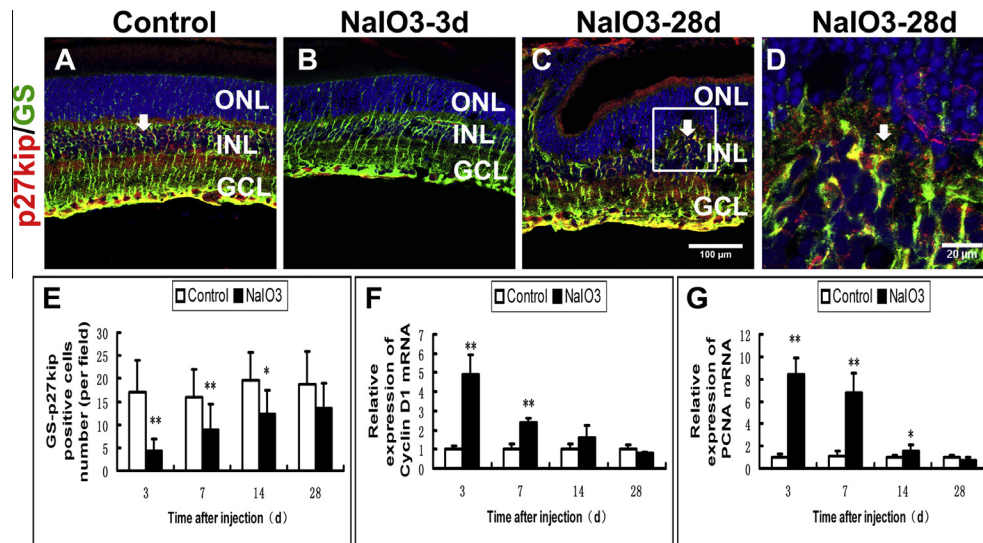
Fig. 6. Results of NaIO$_3$ administration in downregulated p27^{Kip1} and upregulated transcript levels of *Cyclin D1* and *PCNA*. Double-labeling immunofluorescence staining was performed on frozen retinal tissue sections treated with NaIO$_3$ and with GS (green) and p27^{Kip1} (red). PBS-treated retinal tissues are used as controls. The expression of p27^{Kip1} in the INL was consistent with Müller cells, which were indicated by GS immunoreactivity. (A) Shows high p27^{Kip1} expressions in Müller cells in control retinas. (B) Shows a dramatic decrease in the proportion of p27^{Kip1}-immunoreactive Müller cells on the 3rd day, and (E) shows a continuous gradual rise on the 7th, 14th and 28th (C) day; which is still lower than the control retinas. The arrow in (D) shows highly magnified p27^{Kip1}-positive Müller's cells. (F) Shows a significant increase in *Cyclin D1* mRNA expression levels in NaIO$_3$-treated rats' retinas; and reached its peak on the 7th day after injury, compared with the control retinas. Thereafter, a progressive decrease in *Cyclin D1* mRNA level occurred with time. (G) Shows the expression patterns of *PCNA* mRNA at all time-points after NaIO$_3$ administration, which are similar to that of the *Cyclin D1* mRNA. ONL: outer nuclear layer; INL: inner nuclear layer; GCL: ganglion cell layer; arrows indicate double positive cell labeling; $n = 18$, *$P < 0.05$, **$P < 0.01$; scale bar = 100/20 μm. (For interpretation of the references to color in this figure legend, the reader is referred to the web version of this article.)

3.9. Notch family molecules and their ligands were transiently downregulated following NaIO$_3$-induced retinal injury

We examined the expression of Notch family molecules and their primary ligand, Delta, which are linked to eye morphogenesis (Cagan & Ready, 1989; Parks, Turner, & Muskavitch, 1995). Immunofluorescence staining revealed that Notch1 (Fig. 8A–C and I, enlarged in D), and Delta (Fig. 8E–G and J, enlarged in H) were primarily localized to the INL and co-localized in the soma or nucleus of Müller cells. In comparison, we noted that these two molecules were significantly downregulated after NaIO$_3$ administration, compared with control retinas (Fig. 8I and J). Interestingly, on the 28th day after NaIO$_3$ administration, Notch1 and its ligand, Delta, showed stronger immunoreactivity compared with other time-points. Western blotting results revealed that the protein expression level of Notch1 was at its lowest on the 3rd day after NaIO$_3$ administration. Thereafter, the expression levels of Notch1 were lower at all time-points in NaIO$_3$-treated retinas, compared with control retinas. However, Notch1 expression levels trended an increase over time. On the 28th day after NaIO$_3$ administration, no significant difference was observed between the two groups (Fig. 8K and L). Similar expression patterns were seen in *Hes1*, a target gene of Notch1, at mRNA level through quantitative RT-PCR (Fig. 8M).

There was no statistical difference between the retinas of the untreated and PBS-treated rats. Therefore, we chose the PBS-treated rats as a control for statistical analysis, which would be compared with the NaIO$_3$-treated group. Similarly, no notable differences were seen among time-matched groups from 3rd to 28th day over a one month period in PBS-treated rats. Therefore, we only showed one immunofluorescence image (3rd day) for the four control groups. For the NaIO$_3$ group, we only showed noticeable immunofluorescence images on the 3rd, 7th or 28th day after treatment. Figures were not shown for other days.

4. Discussion

In this study, we found that retinal Müller cells were activated to undergo fate switching, including transient proliferation, dedifferentiation, and neurogenesis, during the first 3–7 days after NaIO$_3$ administration in rats. These findings were accompanied by a transient increase of NGF signaling and a decrease of Notch signaling.

In higher vertebrates, after injury, Müller cells possess progenitor cell properties and can form new neurons (Karl & Reh, 2010; Takeda et al., 2008). However, this regenerating ability is limited. Following a low dose administration of NaIO$_3$ (15 mg/kg) in mice, endogenous Müller cells proliferated and migrated toward the RPE layer, regenerated the damaged RPE, and restored retinal function; through the overproduction of neurotropic factors (NTs) on the 3rd month of post-injury (Machalinska et al., 2013). In our study, we also observed the dedifferentiation and neurogenesis of mammalian Müller glial cells after NaIO$_3$-induced retinal injury. This observation was due to the fact that Müller cells markedly expressed cell proliferation markers, including BrdU and PH3; stem cell/progenitor cell markers, including SOX2 and PAX6; and photoreceptor markers, such as crx, rhodopsin. However, differently from the case of low dose NaIO$_3$ treatment, an intermediate dose (50 mg/kg) severely and permanently damaged the retina, resulting in the activation of Müller cells. This result caused the Müller cells to undergo a switch in fate, including a transient dedifferentiation, proliferation, and neurogenesis (re-differentiating and producing new specific retinal types of neurons that were destroyed) between 3 and 7 days post-injury. However, we found that a short-lived repair progress could not stop degenerated development and glial scar formation. These data were confirmed by a long-term study (Enzmann et al., 2006) that revealed no behavioral and anatomical recovery up to 6 months post-treatment with an intermediate dose of NaIO$_3$ (50 mg/kg). Therefore,
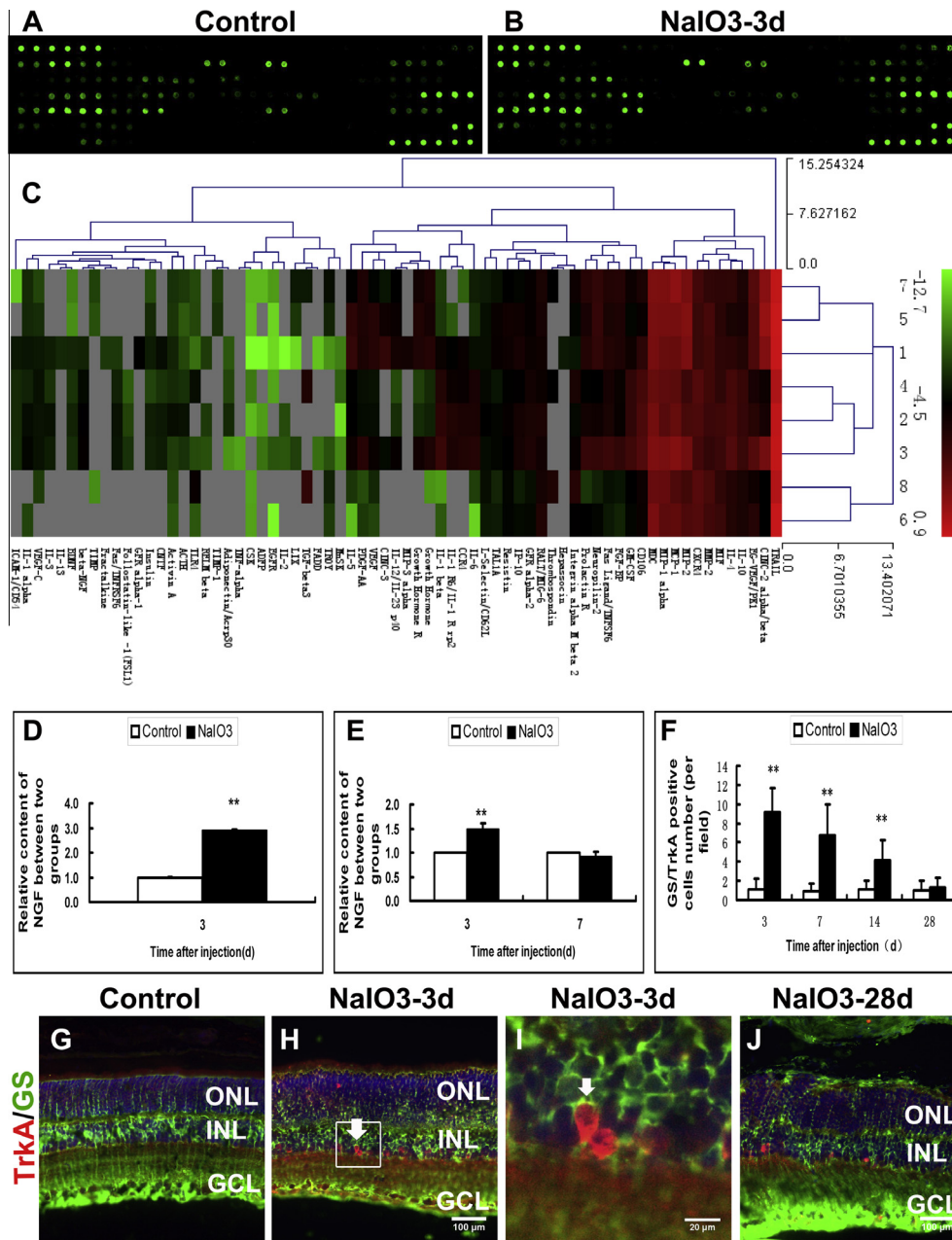
Fig. 7. Results of NaIO$_3$ administration in the short-lived production and release of NGF, and the persistent TrkA upregulation in Müller cells. (A–C) Shows the protein expression profile analysis of retinas treated with NaIO$_3$ or PBS using a RayBiotech array assay. (D) Shows that NGF expression transiently increased in NaIO$_3$-treated retinas, which was only found on the 3rd day of post-injury. On the 7th day after NaIO$_3$ administration, the NGF expression level significantly decreased, which was even lower than the control retinas. The result was further verified by ELISA (E). (G–J) Shows double-labeling immunofluorescence staining with antibodies against GS and TrkA. The results revealed that a portion of TrkA positive signals colocalize with GS-expressing Müller cells. (F) Shows that the number of double positive signals significantly increased in NaIO$_3$ treated retinas, compared with the control retinas; and reached its peak on the 3rd day after NaIO$_3$ administration. Then, the number of double positive Müller cells gradually decreased. ONL: outer nuclear layer; INL: inner nuclear layer; GCL: ganglion cell layer; arrows indicate double positive cell labeling; $n = 18$, $^*P < 0.05$, $^{**}P < 0.01$; scale bar = 100/20 μm.

we hypothesize that a different mechanism of Müller cell dedifferentiation occurred based on different patterns of retinal injury.

At the retinal hyperplasia sites, we found that BrdU was incorporated into the nuclear DNA of some Müller cells. To expel the possibility that Müller cells were simply repairing their DNA, we detected the expression of mitosis marker PH3. The results showed that NaIO$_3$ administration led to the expression of PH3 in some Müller cells. At the same time, we observed an increase in *PCNA* transcript levels. All of these results indicate that Müller cells were replicating rather than repairing their DNA in response to NaIO$_3$-induced retinal injury. In other words, Müller cells re-entered the

cell-cycle. We also noted that after NaIO$_3$ administration, the level of expression of *Cyclin D1* increased and the protein levels of p27^{kip1} decreased. The p27^{kip1} protein inhibits cell cycle progression at G1 by interacting with Cyclin-CDK2 and -CDK4 suppressing *Cyclin D1*. It was noted in a previous study that Müller cell proliferation in adult mouse retinas could also be stimulated by the inactivation of p27^{Kip1} a cyclin-dependent kinase inhibitor (Vazquez-Chona et al., 2011). Therefore, p27^{Kip1} downregulation is considered to be the earliest indicator of Müller glial cell activation (Dyer & Cepko, 2000). Damaged retinal cells are known to be able to release one or more NTs that could stimulate stem cells to enter the
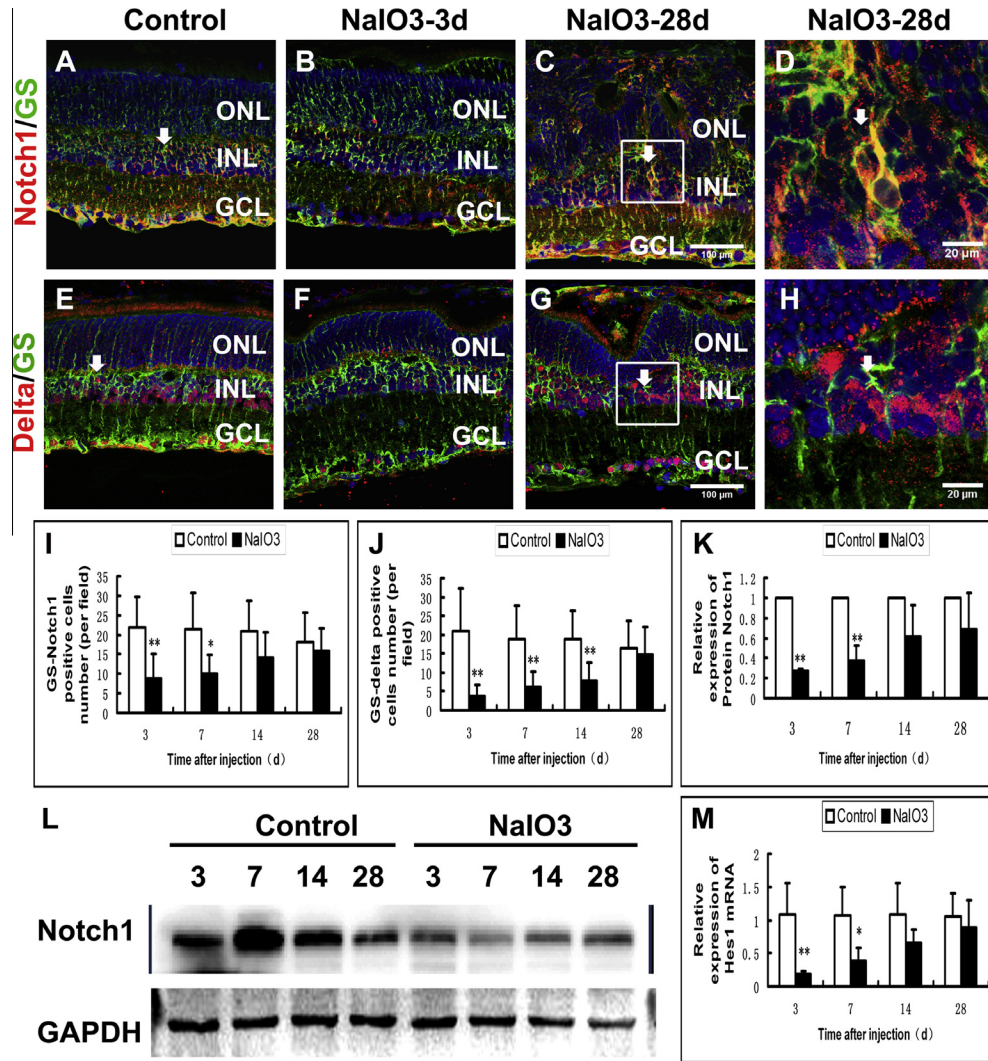
Fig. 8. Results of NaIO$_3$ administration in the rapid decrease of Notch receptors, ligands, and target genes expressions that gradually increase over time. Double-labeling immunofluorescence staining was performed on frozen retinal tissue sections treated with NaIO$_3$ with GS (green), Notch1 (red) or Delta (red). PBS-treated retinal tissues were used as controls. Immunofluorescence staining revealed that Notch1 (A–D) and Delta (E–H) are primarily localized to the INL and are co-localized in the soma or nucleus of Müller cells. Both molecules rapidly downregulated 3rd day after NaIO$_3$ administration, compared with control retinas; which then gradually increased (I and J). Up to the 28th day after NaIO$_3$ administration, Notch1 receptor and its ligand Delta showed stronger immunoreactivity, compared with other time-points after NaIO$_3$ administration (C and G). The arrows in (D) and (H) show highly magnified Notch1 and Delta positive Müller cells, respectively. By Western blotting, (K) and (L) shows the lowest expression level of Notch1, which reduced on the 3rd day after NaIO$_3$ administration. Thereafter, the expression levels of Notch1 decreased at all time-points in NaIO$_3$-treated retinas, compared with control retinas. However, Notch1 expression levels exhibited an increasing trend with time. Up to the 28th day after NaIO$_3$ administration, no significant difference was observed between the two groups. (M) Shows that the expression patterns of the Notch target gene, *Hes1* mRNA, is similar to that of the Notch family at all time-points after NaIO$_3$ administration by quantitative RT-PCR. ONL: outer nuclear layer; INL: inner nuclear layer; GCL: ganglion cell layer; arrows indicate double positive cell labeling; *n* = 18, *$P < 0.05$, **$P < 0.01$; scale bar = 100/20 μm. (For interpretation of the references to color in this figure legend, the reader is referred to the web version of this article.)

cell-cycle by suppressing p27^{kip1} through PI3K/Akt; influencing the survival, migration, adhesion, self-renewal, and differentiation of stem cells (Kayampilly & Menon, 2009; Li et al., 2003; Li et al., 2008; Munugalavadla et al., 2014). Based on this, we found a significant transient overproduction of NGF and NGF-receptor, TrkA, in retinas immediately following NaIO$_3$ administration. Therefore, we believe that NGF/TrkA signaling could transiently stimulate Müller cells to re-enter the cell cycle, dedifferentiating into retinal precursors by suppressing p27^{kip1} and accentuating *Cyclin D1* during the earliest stages of post-NaIO$_3$-induced retinal injury. Seven days later, the number of dedifferentiated Müller cells markedly decreased, as NGF/TrkA signaling decreased.

Recently, many reports (Del Debbio et al., 2010; Fischer & Bongini, 2010; Ghai, Zelinka, & Fischer, 2010) have shown that Notch signaling is involved in Müller cell regulation after injury

and that Notch may alter the capacity of dedifferentiated Müller cells to enter a neurogenic progenitor cell state. In this study, we also detected Notch signaling molecules and found a transiently reduced expression of Notch1 and Delta in Müller cells. We hypothesize that the transient suppression of Notch signaling is extremely and meaningfully in agreement with previous reports.

Notch1, a cell-surface receptor may upregulate the Hes (hairy and enhancer of split) class of genes by interacting with the ligand Delta that releases the Notch intracellular domain which activates the CSL complex consisting of CBF-1, suppressor of hairless and Lag-1. *Hes1* is a crucial transcriptional repressor that inhibits the expression of differentiation-promoting genes, including bHLH (basic helix-loop-helix) (Ahmad et al., 2004). Previous studies have confirmed that endogenous Hes1 was also a component of the NGF signaling pathway; and that Hes1 DNA-binding activities are

inhibited post-translationally during NGF signaling (Strom et al., 1997). During the early stages of NaIO$_3$-induced retinal injury, the decreased activation of the Notch pathway, cooperated with the upregulation NGF signaling, depressed the expression of Hes1; thereafter promoting bHLH transcription. Upregulated bHLH sequesters the transcriptional co-activator CBP/p300 needed for the activation of glial-specific STAT-mediated genes, preventing premature gliogenesis and simultaneously encourages stem cells to differentiate into neurons (Ahmad et al., 2004; Jadhav, Mason, & Cepko, 2006; James et al., 2004). In this injury model, the transient Notch1 downregulation and NGF upregulation promote dedifferentiated Müller cells to differentiate into photoreceptors in a 3-day post-injury photoreceptor-degenerative microenvironment. As time went on, NGF downregulation and Notch1 upregulation depressed the neurogenesis of Müller cells and promoted them to proliferate for a longer period of time; eventually taking on a glial fate. In fact, gliosis is important for protecting and repairing retinal neurons. Müller cell gliosis limits excitotoxic damage and provides neuroprotection in the NaIO$_3$-induced injury model; but excessive Müller glial cell hyperplasia may result to an imbalance between pro-angiogenic and anti-angiogenic factors leading to the breakdown of the blood–retinal barrier and exacerbating photoreceptor and RPE apoptosis. In addition, excessive Müller glial cell hyperplasia may form a compact network and physically block neurite regrowth through the scar.

These data suggests that Müller cell biological events in response to acute stress, such as transient proliferation, dedifferentiation, neurogenesis, or even final glial scar formation, are determined by gene expression changes. The absence of NGF signaling and the activation of the Notch signaling pathway are related in blocking the repair mechanisms associated within the injured retina of higher vertebrates. Our results suggest that increasing the production and secretion of NGF, and inhibiting the Notch signaling pathway activity by novel strategies, could be a potential therapeutic approach for overcoming Müller gliosis, and delay the progression to blindness and/or treatment of retina-related diseases; wherein, current conventional therapeutic strategies are still ineffective.

Acknowledgments

Appendix A. Supplementary data

Supplementary data associated with this article can be found, in the online version, at http://dx.doi.org/10.1016/j.visres.2015.01.030.

References

Ahmad, I., Das, A. V., James, J., Bhattacharya, S., & Zhao, X. (2004). Neural stem cells in the mammalian eye: types and regulation. *Seminars in Cell & Developmental Biology, 15*, 53–62.

Bernardos, R. L., Barthel, L. K., Meyers, J. R., & Raymond, P. A. (2007). Late-stage neuronal progenitors in the retina are radial Muller glia that function as retinal stem cells. *Journal of Neuroscience, 27*, 7028–7040.

Blackshaw, S., Harpavat, S., Trimarchi, J., Cai, L., Huang, H., Kuo, W. P., et al. (2004). Genomic analysis of mouse retinal development. *PLoS Biology, 2*, E247.

Bringmann, A., Pannicke, T., Grosche, J., Francke, M., Wiedemann, P., Skatchkov, S. N., et al. (2006). Muller cells in the healthy and diseased retina. *Progress in Retinal and Eye Research, 25*, 397–424.

Cagan, R. L., & Ready, D. F. (1989). Notch is required for successive cell decisions in the developing Drosophila retina. *Genes & Development, 3*, 1099–1112.

Del Debbio, C. B., Balasubramanian, S., Parameswaran, S., Chaudhuri, A., Qiu, F., & Ahmad, I. (2010). Notch and Wnt signaling mediated rod photoreceptor regeneration by Muller cells in adult mammalian retina. *PLoS ONE, 5*, e12425.

Dyer, M. A., & Cepko, C. L. (2000). Control of Muller glial cell proliferation and activation following retinal injury. *Nature Neuroscience, 3*, 873–880.

Enzmann, V., Row, B. W., Yamauchi, Y., Kheirandish, L., Gozal, D., Kaplan, H. J., et al. (2006). Behavioral and anatomical abnormalities in a sodium iodate-induced model of retinal pigment epithelium degeneration. *Experimental Eye Research, 82*, 441–448.

Fariss, R. N., Li, Z. Y., & Milam, A. H. (2000). Abnormalities in rod photoreceptors, amacrine cells, and horizontal cells in human retinas with retinitis pigmentosa. *American Journal of Ophthalmology, 129*, 215–223.

Fischer, A. J., & Bongini, R. (2010). Turning Muller glia into neural progenitors in the retina. *Molecular Neurobiology, 42*, 199–209.

Fischer, A. J., & Reh, T. A. (2001). Muller Glia are a potential source of neural regeneration in the postnatal chicken retina. *Nature Neuroscience, 4*, 247–252.

Fletcher, E. L. (2000). Alterations in neurochemistry during retinal degeneration. *Microscopy Research and Technique, 50*, 89–102.

Ghai, K., Zelinka, C., & Fischer, A. J. (2010). Notch signaling influences neuroprotective and proliferative properties of mature Muller Glia. *Journal of Neuroscience, 30*, 3101–3112.

Goldman, D. (2014). Muller glial cell reprogramming and retina regeneration. *Nature reviews Neuroscience, 15*, 431–442.

Huo, S. J., Li, Y. C., Xie, J., Li, Y., Raisman, G., Zeng, Y. X., et al. (2012). Transplanted olfactory ensheathing cells reduce retinal degeneration in Royal College of Surgeons rats. *Current Eye Research, 37*, 749–758.

Jadhav, A. P., Mason, H. A., & Cepko, C. L. (2006). Notch 1 inhibits photoreceptor production in the developing mammalian retina. *Development, 133*, 913–923.

James, J., Das, A. V., Rahnenfuhrer, J., & Ahmad, I. (2004). Cellular and molecular characterization of early and late retinal stem cells/progenitors: Differential regulation of proliferation and context dependent role of Notch signaling. *Journal of Neurobiology, 61*, 359–376.

Jian, Q., Li, Y., & Yin, Z. Q. (2015). Rat BMSCs initiate retinal endogenous repair through NGF/TrkA signaling. *Experimental Eye Research, 132*, 34–47.

Jian, Q., Xu, H., Xie, H., Tian, C., Zhao, T., & Yin, Z. (2009). Activation of retinal stem cells in the proliferating marginal region of RCS rats during development of retinitis pigmentosa. *Neuroscience Letters, 465*, 41–44.

Karl, M. O., & Reh, T. A. (2010). Regenerative medicine for retinal diseases: activating endogenous repair mechanisms. *Trends in Molecular Medicine, 16*, 193–202.

Kayampilly, P. P., & Menon, K. M. (2009). Follicle-stimulating hormone inhibits adenosine 5′-monophosphate-activated protein kinase activation and promotes cell proliferation of primary granulosa cells in culture through an Akt-dependent pathway. *Endocrinology, 150*, 929–935.

Kimura, H., Spee, C., Sakamoto, T., Hinton, D. R., Ogura, Y., Tabata, Y., et al. (1999). Cellular response in subretinal neovascularization induced by bFGF-impregnated microspheres. *Investigative Ophthalmology & Visual Science, 40*, 524–528.

Kiuchi, K., Yoshizawa, K., Shikata, N., Moriguchi, K., & Tsubura, A. (2002). Morphologic characteristics of retinal degeneration induced by sodium iodate in mice. *Current Eye Research, 25*, 373–379.

Li, Y., Atmaca-Sonmez, P., Schanie, C. L., Ildstad, S. T., Kaplan, H. J., & Enzmann, V. (2007). Endogenous bone marrow derived cells express retinal pigment epithelium cell markers and migrate to focal areas of RPE damage. *Investigative Ophthalmology & Visual Science, 48*, 4321–4327.

Li, B., Chang, C. M., Yuan, M., McKenna, W. G., & Shu, H. K. (2003). Resistance to small molecule inhibitors of epidermal growth factor receptor in malignant gliomas. *Cancer Research, 63*, 7443–7450.

Li, M., Chiu, J. F., Gagne, J., & Fukagawa, N. K. (2008). Age-related differences in insulin-like growth factor-1 receptor signaling regulates Akt/FOXO3a and ERK/Fos pathways in vascular smooth muscle cells. *Journal of Cellular Physiology, 217*, 377–387.

Li, Y., Li, C., Chen, Z., He, J., Tao, Z., & Yin, Z. Q. (2012). A microRNA, mir133b, suppresses melanopsin expression mediated by failure dopaminergic amacrine cells in RCS rats. *Cellular Signalling, 24*, 685–698.

Li, Z. Y., Possin, D. E., & Milam, A. H. (1995). Histopathology of bone spicule pigmentation in retinitis pigmentosa. *Ophthalmology, 102*, 805–816.

Los, M., Maddika, S., Erb, B., & Schulze-Osthoff, K. (2009). Switching Akt: From survival signaling to deadly response. *BioEssays, 31*, 492–495.

Machalinska, A., Kawa, M. P., Pius-Sadowska, E., Roginska, D., Klos, P., Baumert, B., et al. (2013). Endogenous regeneration of damaged retinal pigment epithelium following low dose sodium iodate administration: An insight into the role of glial cells in retinal repair. *Experimental Eye Research, 68*–78.

Machalinska, A., Lubinski, W., Klos, P., Kawa, M., Baumert, B., Penkala, K., et al. (2010). Sodium iodate selectively injuries the posterior pole of the retina in a dose-dependent manner: Morphological and electrophysiological study. *Neurochemical Research, 35*, 1819–1827.

Munugalavadla, V., Mariathasan, S., Slaga, D., Du, C., Berry, L., Del Rosario, G., et al. (2014). The PI3K inhibitor GDC-0941 combines with existing clinical regimens for superior activity in multiple myeloma. *Oncogene, 33*, 316–325.

Nelson, C. M., Ackerman, K. M., O'Hayer, P., Bailey, T. J., Gorsuch, R. A., & Hyde, D. R. (2013). Tumor necrosis factor-alpha is produced by dying retinal neurons and is required for Muller Glia proliferation during zebrafish retinal regeneration. *Journal of Neuroscience, 33*, 6524–6539.

Nguyen, T., Nioi, P., & Pickett, C. B. (2009). The Nrf2-antioxidant response element signaling pathway and its activation by oxidative stress. *Journal of Biological Chemistry, 284*, 13291–13295.

Ooto, S., Akagi, T., Kageyama, R., Akita, J., Mandai, M., Honda, Y., et al. (2004). Potential for neural regeneration after neurotoxic injury in the adult mammalian retina. *Proceedings of the National Academy of Sciences of the United States of America, 101*, 13654–13659.

Parks, A. L., Turner, F. R., & Muskavitch, M. A. (1995). Relationships between complex Delta expression and the specification of retinal cell fates during Drosophila eye development. *Mechanisms of Development, 50*, 201–216.

Paul, S. (2008). Dysfunction of the ubiquitin-proteasome system in multiple disease conditions: Therapeutic approaches. *BioEssays, 30*, 1172–1184.

Pierce, E. A., Quinn, T., Meehan, T., McGee, T. L., Berson, E. L., & Dryja, T. P. (1999). Mutations in a gene encoding a new oxygen-regulated photoreceptor protein cause dominant retinitis pigmentosa. *Nature Genetics, 22*, 248–254.

Rich, K. A., Figueroa, S. L., Zhan, Y., & Blanks, J. C. (1995). Effects of Muller cell disruption on mouse photoreceptor cell development. *Experimental Eye Research, 61*, 235–248.

Strom, A., Castella, P., Rockwood, J., Wagner, J., & Caudy, M. (1997). Mediation of NGF signaling by post-translational inhibition of HES-1, a basic helix-loop-helix repressor of neuronal differentiation. *Genes & Development, 11*, 3168–3181.

Takeda, M., Takamiya, A., Jiao, J. W., Cho, K. S., Trevino, S. G., Matsuda, T., et al. (2008). Alpha-aminoadipate induces progenitor cell properties of Muller Glia in adult mice. *Investigative Ophthalmology & Visual Science, 49*, 1142–1150.

Tao, Z., Dai, J., He, J., Li, C., Li, Y., & Yin, Z. Q. (2013). The influence of NaIO(3)-induced retinal degeneration on intra-retinal layer and the changes of expression profile/morphology of DA-ACs and mRGCS. *Molecular Neurobiology, 47*, 241–260.

Taomoto, M., Nambu, H., Senzaki, H., Shikata, N., Oishi, Y., Fujii, T., et al. (1998). Retinal degeneration induced by N-methyl-N-nitrosourea in Syrian golden hamsters. *Graefes Archive for Clinical and Experimental Ophthalmology, 236*, 688–695.

Vazquez-Chona, F. R., Swan, A., Ferrell, W. D., Jiang, L., Baehr, W., Chien, W. M., et al. (2011). Proliferative reactive gliosis is compatible with glial metabolic support and neuronal function. *BMC Neuroscience, 12*, 98.

Wan, J., Zheng, H., Xiao, H. L., She, Z. J., & Zhou, G. M. (2007). Sonic hedgehog promotes stem-cell potential of Muller glia in the mammalian retina. *Biochemical and Biophysical Research Communications, 363*, 347–354.

Weng, N. P., Araki, Y., & Subedi, K. (2012). The molecular basis of the memory T cell response: Differential gene expression and its epigenetic regulation. *Nature Reviews Immunology, 12*, 306–315.

WHO (2007). *Diabetes facts*, 805–816. Available at: http://www.who.int/mediacentre/factsheets/fs312/en/index.html> Accessed 13.12.07.

Xu, Y., Chen, C., Jin, N., Zhu, J., Kang, L., Zhou, T., et al. (2013). Muller Glia cells activation in rat retina after optic nerve injury: Spatiotemporal correlation with transcription initiation factor IIB. *Journal of Molecular Neuroscience*, 37–46.